List of Abbreviations

Abbreviation	*Full form*
2D	Two-dimensional
TMDs	Transition Metal Dichalcogenides
JTMDs	Janus Transition Metal Dichalcogenides
LDA	Local Density Approximation
GGA	Generalized Gradient Approximation
mBJ	Modified Becke-Johnson
PBE	Perdew-Burke-Ernzerhof
SCF	Self-Consistent Field
DFT	Density Functional Theory
DFPT	Density Functional Perturbation Theory
BZ	Brillouin zone
BoltzTraP	Boltzmann Transport
QE	Quantum ESPRESSO
ESPRESSO	opEn Source Package for Research in Electronic Structure, Simulation, and Optimization
DOS	Density of States
TDOS	Total Density of States
PDOS	Projected Density of States
SPDOS	Spin Polarized Density of States
HOMO	Highest Occupied Molecular Orbital
LUMO	Lowest Unoccupied Molecular Orbital
CDD	Charge Density Difference
SCAPS-1D	One Dimensional Solar Cell Capacitance Simulator
CVD	Chemical Vapor Deposition
SOC	Spin Orbit coupling
STEM	Scanning Tunneling Electron Microscopy
AZO	Aluminum doped Zinc Oxide
QE	Quantum Efficiency
vdW	Van der Waals
VBM	Valence Band Maximum
CBM	Conduction Band Minimum
VB	Valence Band
CB	Conduction Band
TCO	Transparent Conducting Oxide
PV	Photovoltaic
CTC	Cumulative lattice Thermal Conductivity

Declaration

I hereby declare that the work presented in this Thesis titled "*Low Dimensional Transition Metal Dichalcogenides for Nano Device Applications*" submitted to the Indian Institute of Technology Jodhpur in partial fulfilment of the requirements for the award of the degree of Doctor of Philosophy, is a bonafide record of the research work carried out under the supervision of Dr. Ambesh Dixit. The contents of this thesis in full or in parts, have not been submitted to, and will not be submitted by me to, any other Institute or University in India or abroad for the award of any degree or diploma.

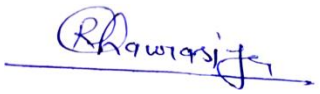

Rajneesh Chaurasiya

P16PH001

Certificate

This is to certify that the thesis titled "*Low Dimensional Transition Metal Dichalcogenides for Nano Device Applications*", submitted by *Rajneesh Chaurasiya* (*P16PH001*) to the Indian Institute of Technology Jodhpur for the award of the degree of *Doctor of Philosophy*, is a bonafide record of the research work done by him under my supervision. To the best of my knowledge, the contents of this report, in full or in parts, have not been submitted to any other Institute or University for the award of any degree or diploma.



Ambesh Dixit

Ph.D. Thesis Supervisor

Acknowledgements

First and foremost, I would like to express sincerest gratitude to my supervisor Dr. Ambesh Dixit for considering me as a PhD student at IIT Jodhpur. He motivated me a lot with his brilliant knowledge and incredible discussion that made my PhD life simpler. I truly admire his professional guidance towards the science and approach to deal with different objectives. He has provided me a freedom and great platform for research and without his excellence, wisdom and careful supervision this work would never be completed.

I offer my gratitude and deep sense of appreciation to my M. Tech thesis supervisor Dr. Rajnish Kurchania (NIT Bhopal), Prof. Sampat Raj Vadera (IITJ) and doctoral committee member Dr. Satyajit Sahu (IITJ), Dr. Ashutosh Kumar Alok (IITJ), Dr. Shree Prakash Tiwari (IITJ) for their constructive criticism, suggestions and being so patient with me that help to improve my research work.

I would like to thank collaborators Prof. Ravindra Pandey (MTU, USA), Prof. Sushil Auluck (NPL, Delhi), and Dr. Nirpendra Singh (KUST, UAE) for fruitful discussion and encouragement during the research activities whenever needed.

My heartfelt respect to seniors Dr. Belal Usmani, Dr. Lokesh Saini, Dr. Rohitash Kumar, Dr. Goutam Kumar Gupta, Dr. Anurag Sahu, Dr. Rajesh Kumar Jha, Dr. Chandni Kumari and Dr. Sudipto Som for their encouragement and making me familiar with the research environment. I am also thankful to my friends Mr. Abhijeet J. kale, Mr. Chandra Prakash, Mr. Sumit Kukreti, Mr. Ajay Tiwari, Mr. Ram Milan Sahani, Mr. Radha Raman, Mr. Shubham Tyagi, Mr. Nilesh Kumar, Mr. Dushmant Naik, and Mr. Lwithwsa Swargiary for making my life joyful at IIT Jodhpur. I also extend my thanks to all my friends and staff at IIT Jodhpur.

I also gratefully acknowledge to all scientist and professor who helped me, providing research guidance & support during my research work. My acknowledgement also extends to all those people, apart from aforementioned whom I was fortunate enough to meet with, during this journey and who enriched me with their support and knowledge.

My special thanks to the Ministry of Human Resource Development (MHRD), the Government of India for providing me financial support during my stay at IIT Jodhpur. I acknowledge IIT Jodhpur for providing me an experimental and computational facility. I offer my humble thanks to the Ministry of Education (MOE), Taiwan, and Professor Chung Hsin Lu (NTU Taiwan) for providing me the internship opportunity.

I dedicate this thesis to my grandfather, late Mr. Ramgopal Chaurasiya. He was my first teacher and the foundation builder of my carrier. I am thankful for the unconditional support and sacrifices of my parents Mr. Ashok Chaurasiya, and Ms. Sumitra Chaurasiya made me on my behalf. I don't have a word to express how thankful I am to my elder brothers Mr. Rajesh Kumar Chaurasiya and Anand Kumar Chaurasiya. I am grateful to my sisters Ms. Rajnee Chaurasiya and Ms. Sangeeta Chaurasiya.

Rajneesh Chaurasiya
PhD Student

List of Figures

Figures	*Title*	*page*
1.1	(a) Top view, (b) side view and (c) band structure along high symmetry points of BZ of graphene.	2
1.2	Schematic representations of few selected 2D monolayers and corresponding electronic band gap	3
2.1	Periodic table representing the possible transition metals and chalcogen atoms, top view of hexagonal and trigonal phase and corresponding possible symmetry	6
2.2	Band gap variation of monolayer, bilayer, trilayer and quad layer of WS_2 without and with SOC.	8
2.3	Schematic representation of (a) light absorption and photoluminescence, and (b) Raman scattering.	9
2.4	Band gap variation against the uniaxial and biaxial strain of MX_2 (M = Mo, W; X = S, Se and Te) monolayers	10
2.5	Point defects and antisite defects observed in MoS_2 monolayer using the STM analysis	10
2.6	Schematic representation of applications of TMDs based monolayers	11
2.7	(a) Steps used for synthesis process, (b) Raman spectrum, (c) Photoluminescence spectrum and (d) Angular dark field STEM of MoSSe monolayer	12
2.8	Theoretically explored applications of JTMDs monolayers.	13
3.1	Density functional theory based per year publications from 2000 to 2019 (Source: Web of Science)	15
3.2	Schematic representation of Schrödinger system for electrons and nuclei interaction	16
3.3	Jacob's ladder of exchange correlation functional	19
3.4	Flow chart of self-consistent field cycle iteration	20
3.5	Schematic representation of approximation of full potential to pseudopotentials	21
3.6	Flow chart diagram of Density Functional Perturbation Theory	23
4.1	Optimized geometries and corresponding structural parameters of (a) WS_2, (b) WSSe and (c) WSe_2 monolayer; (d) Schematic representation of hexagonal BZ.	27
4.2	Schematic representation of vibrational modes of WS_2 monolayer	27
4.3	Phonon band dispersion of (a) WS_2, (b) WSSe, and (c) WSe_2 monolayer	28
4.4	(a), (c) and (e) are the band structure and (b), (d) and (f) are the PDOS of WS_2, WSSe and WSe_2 monolayers, respectively.	28
4.5	Band structure of (a) WS_2, (b) WSSe, and (c) WSe_2 monolayers using GGA+SOC	29
4.6	Phonon band dispersion (a) 6% compressive strain (b) 2% compressive strain (c) 2% tensile strain and (d) 6% tensile strain for WSSe monolayer	29
4.7	Electronic band structure of (a) and (b) at 1.5% compression strain and 0.5% tensile strain, WS_2 monolayer, respectively; (c) and (d) 1 % compression strain and 1% tensile strain, WSSe monolayer, respectively; (e) and (f) at 1.5% compression strain at 2.5% tensile strain, WSe_2 monolayer, respectively.	30
4.8	(a) Band gap, (b) effective mass and (c) mobility variation of WS_2, WSSe and WSe_2 monolayers.	31
5.1	Schematic representation of initial geometry of H_2S, NH_3, NO_2 and NO molecules	34
5.2	(a) and (b) are the band structure; (c) and (d) are PDOS of WSSe@Ses and WSSe@Sse monolayer, respectively.	35
5.3	Optimized structures of H_2S (a–d), NH_3 (e–h), NO_2 (i–l) and NO (m–p) molecules adsorbed on the selenium and sulfur surfaces of the WSSe monolayer.	36
5.4	(a-d) H_2S, (e-h) NH_3, (i-l) NO_2 and (m-p) NO charge density difference.	37
5.5	Comparison of SPDOS of pristine monolayer and molecule adsorbed monolayers (a&b) H_2S, (c&d) NH_3, (e&f) NO_2 and (g-h) NO	38
5.6	(a) Adsorption energy and (b-d) temperature dependent recovery times of molecules adsorb on selenium and sulfur surface of monolayer.	38
5.7	(a-d) Optimized geometries, (e-h) charge density difference and (i-l) SPDOS of gas molecules adsorb on WSSe@Ses monolayer.	40

5.8	(a-d) Optimized geometries, (e-h) charge density difference and (i-l) SPDOS of gas molecules adsorb on WSSe@Sse monolayer.	41
5.9	(a) and (b) are the band structure; (c) and (d) are PDOS of MoSSe@Sev and MoSSe@(S/Se)v monolayer, respectively.	42
5.10	Optimized geometries and charge density difference of H2S adsorb on MoSSe (a&b), NH3 adsorb on MoSSe (c&d), NO2 adsorb on MoSSe (e&f) and NO adsorb on MoSSe (g&h).	43
5.11	Comparison of band structure of pristine monolayer with the gas molecule adsorbs on MoSSe monolayer (a) H2S, (b) NH3, (c) NO2 and NO.	44
5.12	(a) Adsorption energy and (b) vertical height of gas molecules adsorb on pristine MoSSe monolayer	45
5.13	Optimized geometries and charge density difference of H2S (a&b), NH3 (c&d), NO2 (e&f) and NO (g&h) adsorb on MoSSe@Vse monolayer.	46
5.14	Optimized geometries and charge density difference of H2S (a&b), NH3 (c&d), NO2 (e&f) and NO (g&h) adsorb on MoSSe@$V_{(S/Se)}$ monolayer.	47
5.15	Comparison of band structure of pristine monolayer with the gas molecule adsorbs on MoSSe@V_{Se} monolayer (a) H2S, (b) NH3, (c) NO2 and (d) NO.	47
5.16	Comparison of band structure of pristine monolayer with the gas molecule adsorb on MoSSe@ $V_{(S/Se)}$ monolayer (a) H2S, (b) NH3, (c) NO2 and (d) NO.	48
5.17	(a) Adsorption energy and (b) vertical height of gas molecules adsorb on MoSSe@ V_{Se} and MoSSe@ $V_{(S/Se)}$ monolayer.	48
6.1	Schematic diagram and corresponding structural parameters of (a) bulk WS_2 and (b) bulk WSe_2.	52
6.2	(a) Band structure of WS_2 (b) TDOS & PDOS of bulk WS_2 (c) Band structure of WSe_2 and (b) TDOS & PDOS of bulk WSe_2	53
6.3	(a) Band structure of WSSe (b) TDOS & PDOS of WSSe monolayer, (c) band structure of WSeTe and (b) TDOS & PDOS of WSeTe monolayer.	54
6.4	Absorption spectra of bulk WS2, (b) absorption spectra of bulk WSe2 and (c) absorption spectra of WSSe and WSeTe monolayers.	55
6.5	(a) Schematic representation of solar cell device, (b) band alignment at interface (c) J-V curve and (d) EQE of TCO/WSSe/WS_2, TCO/WSeTe/WS_2, TCO/WSSe/WSe_2 and TCO/WSeTe/WSe_2 solar cell devices.	57
6.6	Effect of acceptor layer thickness on (a) efficiency (b) open circuit voltage and (c) short circuit current of TCO/WSSe/WS_2, TCO/WSeTe/WS_2, TCO/WSSe/WSe_2 and TCO/WSeTe /WSe_2 solar cell devices.	58
6.7	Effect of acceptor layer carrier concentration on (a) efficiency (b) open circuit voltage and (c) short circuit current of TCO/WSSe/WS_2, TCO/WSeTe/WS_2, TCO/WSSe/WSe_2 and TCO/WSeTe /WSe_2 solar cell devices.	58
6.8	Contour plot of interface recombination speed at interface versus minority carrier life time of (a) AZO/WSSe/WS_2 (b) AZO/WSeTe/WS2 (c) AZO/WSSe/WSe_2 and (d) AZO/WSeTe/WSe_2 solar cell devices.	59
6.9	Contour plot of an acceptor layer carrier concentration versus thickness of buffer layer of (a) AZO/WSSe/WS_2 (b) AZO/WSeTe/WS_2 (c) AZO/WSSe/WSe_2 and (d) AZO/WSeTe/WSe_2 solar cell devices.	60
6.10	(a) J-V and (b) QE plot based on the optimized parameters of considered solar cells.	61
7.1	Phonon band dispersion curve of Janus WSSe monolayer.	64
7.2	(a) Carrier concentration, (b) density of states, (c) Seebeck coefficient, (d) electrical conductivity, (e) electronic thermal conductivity, (f) lattice thermal conductivity, (g) power factor and (h) figure of merit versus chemical potential of unstrained WSSe monolayer.	65
7.3	Cumulative thermal conductivity versus mean free path of WSSe monolayer at (a) 300K and (b) 1500K.	66
7.4	Comparison of phonon band softening and/or hardening under the compressive and tensile strains. Here K refers Γ-M-K-Γ direction.	68
7.5	Variation of the valence and conduction band edges under the biaxial compressive and tensile strains	68
7.6	Strain dependent Seebeck coefficients for (a) p-type carriers, (b) n-type carriers and (c) band gap and Seebeck coefficient.	69
7.7	Chemical potentials dependent electrical conductivity of WSSe monolayer at different temperatures for (a) – 6%, (b) - 4%, (c) -2%, (d) 2%, (e) 4% and (f) 6% strain.	70

7.8	Chemical potentials dependent electronic thermal conductivity of WSSe monolayer at different temperatures for (a) – 6%, (b) - 4%, (c) -2%, (d) 2%, (e) 4% and (f) 6% strain.	71
7.9	The variation in (a) frequency of LA, TA and ZA modes and group velocity against strain and (b) Lattice thermal conductivity against temperature at different strain values for WSSe monolayer.	72
7.10	Chemical potentials dependent power factor of WSSe monolayer at different temperatures for (a) – 6%, (b) - 4%, (c) -2%, (d) 2%, (e) 4% and (f) 6% strain.	73
7.11	Chemical potentials dependent figure of merit of WSSe monolayer at different temperatures for (a) – 6%, (b) - 4%, (c) -2%, (d) 2%, (e) 4% and (f) 6% strain.	74
7.12	(a) Schematic representation of WSSe monolayer based thermoelectric device, and (b) the comparison of thermoelectric device efficiency against temperature for unstrained and strained WSSe monolayers.	74
8.1	Explored applications of Janus monolayers	78
8.2	The potential future possibilities with Janus monolayers	79

List of tables

Tables	*Title*	*page*
5.1	Comparison of adsorption energy and Bader charge analysis of widely used monolayers	39
6.1	Structural parameters of bulk absorber material and Ultra-thin Janus structures.	52
6.2	Material parameter of absorber, buffer, and TCO materials used to simulate the performance of solar cells	56

List of symbols

Symbol	*Description*
Å	Angstrom (10^{-10} m)
E_g	Electronic band gap
h-BN	Hexagonal boron nitride
τ	Relaxation Time
S	Seebeck coefficient
σ	Electrical conductivity
κ_{el}	Electronic thermal conductivity
ZT	Figure of merit
ρ	Electron density
$\hat{H}$	Hamiltonian
E	Energy
Ψ	Wave function
ϕ_i	Kohn –Sham orbital
eV	Electron Volt
μ	Mobility
η	Efficiency
V_{OC}	Open circuit voltage
I_{SC}	Short circuit voltage
m*	Effective mass
T	Temperature